International Journal of Engineering & Extended Technologies Research (IJEETR)

|ISSN: 2322-0163| www.ijeetr.com | A Bimonthly, Peer Reviewed, Scholarly Indexed Journal |

| Volume 8, Issue 2, March - April 2026 |

DOI:10.15662/IJEETR.2026.0802126

Antenna Array for 5G Applications

Sugumari T, Alageshwari R, Kavitha T S, Dharshini I

Associate Professor, Department of Electronics and Communication Engineering, KLN College of Engineering, Madurai, Tamil Nadu, India

UG Scholars, Department of Electronics and Communication Engineering, KLN College of Engineering, Madurai, Tamil Nadu, India

ABSTRACT: This project presents apatch filtenna integrated with a Cylindrical Dielectric Resonator Antenna (CDRA) array to enable simultaneous microwave and millimeter-wave communication. An elliptical patch antenna is designed for sub-6 GHz operation, with a hollow section to accommodate the CDRA, which resonates in the mm-wave band. The two resonators are combined to ensure seamless dual-band operation. A low-pass filter is incorporated to suppress unwanted harmonics and enhance isolation between bands. The mm-wave DRA is configured as a multi-element array to achieve high realized gain, while the overall design maintains a compact size and wide bandwidth. The proposed antenna demonstrates excellent isolation, independent band control, and high-gain mm-wave radiation suitable for long-distance communication. The main innovation lies in integrating a microwave filtenna with a high-gain mm-wave antenna array, emphasizing filtering for the lower band and enhanced mm-wave performance. The proposed antenna operates at resonant frequencies around **7.46 GHz and 12.83 GHz, corresponding to C-band and Ku-band operation s**and the proposed antenna supports emerging 5G mid-band (FR3) and satellite-based Ku-band applications.

KEYWORDS: Antenna Array, 5G Communications, Beamforming, Massive MIMO, Millimeter Wave, Phased Array, Wireless Networks

I. INTRODUCTION

The rapid evolution of wireless communication systems, driven by emerging technologies such as 5G and beyond, has significantly increased the demand for antennas capable of operating across multiple frequency bands. Modern communication networks require seamless integration of sub-6 GHz microwave frequencies, which provide reliable coverage and penetration, along with millimeter-wave (mm-wave) frequencies that support high data rates and large bandwidth. This dual-band requirement has introduced new challenges in antenna design, particularly in achieving compactness, high efficiency, wide bandwidth, and minimal interference between operating bands.

Traditional antenna systems often rely on separate components to handle different frequency ranges, leading to increased system complexity, larger size, and higher cost. Moreover, coexistence of microwave and mm-wave bands within a single platform introduces issues such as mutual coupling, harmonic distortion, and signal interference, which degrade overall system performance. To address these challenges, recent research has focused on multifunctional antennas that can integrate filtering characteristics directly into the radiating structure, commonly referred to as filtennas. These antennas eliminate the need for external filters, thereby reducing insertion loss, improving selectivity, and enhancing spectral efficiency.

Another important aspect in next-generation communication is the use of dielectric resonator antennas (DRAs), which have gained attention due to their inherent advantages such as high radiation efficiency, low conductor losses, and suitability for high-frequency applications, particularly in the mm-wave spectrum. Additionally, antenna arrays are widely employed to improve gain and directivity, which are essential for overcoming the high propagation losses associated with mm-wave communication.

Despite these advancements, integrating microwave filtering functionality with high-gain mm-wave antenna structures within a single compact design remains a complex task. Key design challenges include achieving effective isolation between bands, maintaining independent control over each frequency range, and ensuring stable radiation characteristics without performance degradation. Therefore, there is a growing need for innovative antenna architecture that can simultaneously support multi-band operation, incorporate filtering capabilities, and deliver high gain, all while maintaining a compact and efficient structure suitable for modern wireless communication systems.

International Journal of Engineering & Extended Technologies Research (IJEETR)

|ISSN: 2322-0163| www.ijeetr.com | A Bimonthly, Peer Reviewed, Scholarly Indexed Journal |

| Volume 8, Issue 2, March - April 2026 |

DOI:10.15662/IJEETR.2026.0802126

II. SURVEY

Li, Y et al proposed an eight-element multiple-input multiple-output (MIMO) antenna array for 5G/WLAN micro wireless access points. The proposed MIMO antenna is formed by integrating eight identical antenna elements. For each array element, four operation bands, namely, LTE bands 42/43 (3400–3800 MHz), 4.9-GHz band (4800–5000 MHz) and 5.2-GHz WLAN (5150–5350 MHz) are fully covered for 8 × 8 MIMO use.

Zou, H et al presented a dual-band 6 × 6 antenna array operating in the LTE band7 downlink (2620–2690 MHz) and LTE band46 (5150– 5925 MHz) for 4.5G/5G communication multi-input multi-output (MIMO) operation in the smartphone . The proposed dual-band antenna array elements are symmetrically placed along the long edges of the smartphone, and the antenna element is composed of three parts

Li, Y., Zou, H., Wang, M., Peng, M., & Yang, G. (2018). A Quad-Band Eight-Antenna Array for 5G/WLAN MIMO in Micro Wireless Access Points. 2018 IEEE International Symposium on Antennas and Propagation & USNC/URSI National Radio Science Meeting.

Hu, H.-N et al proposed a dual linearly-polarized antenna subarray that operates at 28 GHz and 38 GHz for fifth generation (5G) base stations. In contrast to earlier millimeter-wave base-station antennas that implement individual single-band antennas, simultaneous realization of dual-band operation can save space and cost. In addition, the proposed subarray depicts dual polarizations, improving signal reliability through polarization diversity.

Haskou, A presents a novel four-port, broadband, compact MIMO antenna operating in the sub-6GHz bands of future 5G systems and the 2.45GHz/5GHz WiFi bands. The radiating element topology is inspired from both the Annular Slot Antenna (ASA) and the printed wideband monopole. V-shaped slots are incorporated in the antenna ground for better efficiency and higher in-plane radiation. Hussain, N et al presents, the design and the realization of a low-profile, compact, and broadband circularly polarized (CP) Fabry-Perot resonant antenna using a single superstrate for fifth generation (5G) wireless multiple-input-multiple-output (MIMO) applications. The antenna consists of a corner cut patch with a diagonal slot and a superstrate. The individual resonances of the corner cut patch and patch with diagonal slot are overlapped to improve the intrinsic narrow impedance and axial ratio (AR) bandwidths of the single-fed patch antennas

Wang, Y et al presents a small, coplanar waveguide (CPW)-fed wideband antenna for 5G/WLAN application. The proposed antenna consists of a pair of symmetrical meandering C-shaped strips, a rectangular ring strip and a monopole radiator. The designed antenna has a compact size of 20 × 27.5mm2 (0.16λ0 × 0.22λ0). The simulated results show that the proposed antenna has 10-dB impedance bandwidths of 3530 MHz (2.37-5.9 GHz) to cover all the 2.4/5.2/5.8-GHz WLAN bands and the 5G candidate bands (3-6 GHz).

Wang, Y.-Y et al proposed a integrated design of 4G antennas and 5G antennas applied to glasses. The most important highlight of this design is that it makes full use of the limited three-dimensional space structure provided by glasses and achieves the perfect combination of the antenna and glasses in the physical structure. Specifically, two antennas for 4G communication are arranged on two glasses frames, and four antennas for 5G communication are arranged on two glasses legs.

Da Costa, I. F et al reports an innovative structure and preliminary results of a four-elements antenna array with beam steering for 5G access cellular networks, operating in the underutilized millimetre wave (mm-wave) frequency spectrum.

Alja'afreh, S. S et al proposed a self-isolated 10-element antenna array operating in the long-term evolution 42 (LTE42) frequency band for 5G massive MIMO smartphone applications. The proposed antenna elements are placed in a 2D array configuration; they are placed symmetrically along the two long edges of the mobile chassis. The proposed antenna structure is a shorted loop antenna resonating at half-wavelength mode, which is rarely deployed by researchers due to its large size compared to other quarter wavelength antenna structures.

Chen, Y et al presented a single-fed dual-band L-probe fed antenna for 5G applications. The proposed antenna is designed to operate as a dual-band radiator by utilizing the L-shaped probe and stacked patches, and the center of two bands is 28 GHz and 39 GHz, respectively. This antenna features wide-beam at H-plane and wideband characteristics. Furthermore, the beamwidth is approximately 140°at 28GHz and over 180°at 39GHz. The total efficiency of the

|ISSN: 2322-0163| www.ijeetr.com | A Bimonthly, Peer Reviewed, Scholarly Indexed Journal |

| Volume 8, Issue 2, March - April 2026 |

DOI:10.15662/IJEETR.2026.0802126

antenna is over 90% in lower band and about 90% in upper band. The dimensions of the proposed antenna structure are 10mm×10mm× 0.9 mm. The simulation results show the antenna has good impedance and radiation characteristics, which make it suitable for 5G millimeter-wave communication.

Chattha, H. T. et al presented a compact, low-profile four-port, two-element antenna for 5G Internet of Things (IoT) and handheld applications having a height h = 3.0 mm . The antenna structure contains two planar Inverted-F antenna (PIFA) elements having same shape. Each antenna element has two feeding plates placed at right angle to each other to make them cross-polarized for the exploitation of polarization diversity, whereas spatial diversity is employed by positioning two antennas diagonally on opposite sides of the antenna structure. For reducing mutual coupling, etching of rectangular slots on each side of ground plane beneath the top plate of each element has been done to stop the flow of current between two ports of the same antenna element.

Valkonen, R et al presents the design of two 64-element phased array antennas for 5G access, operating at 28 GHz and at 39 GHz frequency bands. The 8x8-element antenna arrays use a multi-layer printed circuit board stack. 16 commercial quad-core TX/RX ICs are used to provide independent control of phase and amplitude for each radiating element. RF power distribution and combining network is integrated on the PCB, with a single RF interface to an external radio transceiver. Analysis and design of the feed network for the antenna elements is demonstrated.

Kim, G et al presents a dual polarized broadband microstrip patch antenna for a 5G mmWave antenna module on an FR4 substrate. The proposed antenna was fabricated using a standard FR4 printed circuit board (PCB) process because of its low cost and ease of mass production. The electrical properties of the FR4 substrate in the 5G mmWave frequency band were also characterized. An air cavity structure was introduced to mitigate the high loss tangent of the FR4 substrate. Capacitive elements such as proximity L-probe feedings and parasitic patches are used to improve the impedance bandwidth of the patch antenna.

Zhu, L et al presented a dual-band 2x2 MIMO antenna for wearable device applications to support the 5G radio frequency allocations at 3.3 - 3.6 and 4.5 - 5 GHz in China. The single antenna unit is composed of a monopole mode and a folded loop mode with a single feed to cover these two bands. Two identical antennas positioned at top and bottom sides of a smart watch sized PCB (40x40mm2) are used to demonstrate the MIMO performance. The simulation results from xFDTD show that these MIMO antennas can achieve over 85 % efficiency, more than 17 dB isolation and 0.02 coefficient correlation at both bands

He, Y et al presents a compact dual-band and dual-polarized millimeter-wave patch antenna array with satisfactory performance on element mutual coupling and beam scanning capabilities. Using capacitive feed technique and stacked configuration with extra parasitic strips, the proposed antenna array is able to achieve a wide operating bandwidth in both the low- and high-bands. In order to reduce the array's footprint, and to enhance the beam scanning performance in both bands, the element spacing is shrunk to less than 0.36 wavelength at 26 GHz.

III. PROPOSED ANTENNA

Antenna design plays a vital role in determining its performance. Microstrip patch antenna is simpler to construct as it provides easy feeding and has low profile when compared to other type of antennas. It has a patch supporting radiation, along with a ground plane and the substrate. In the proposed designs the ground plane is made of copper and Rogers material is used for making the substrate. The patch can be of any shape, here the shape of patch chosen to be rectangle instead of circular because it provides high gain.The antenna has slots within the patch and is provided with an inset feed. The antenna design parameters are calculated using various formulas.To get efficient radiation, a practical rectangular patch width *W* can be givenas,

$$W = \frac{C}{2fr\sqrt{\frac{2}{\varepsilon_r+1}}} \qquad (3.1)$$

International Journal of Engineering & Extended Technologies Research (IJEETR)

|ISSN: 2322-0163| www.ijeetr.com | A Bimonthly, Peer Reviewed, Scholarly Indexed Journal |

| Volume 8, Issue 2, March - April 2026 |

DOI:10.15662/IJEETR.2026.0802126

where *fr*is the antenna's resonant frequency and *c* is the speed of light in vacuum. The effective dielectric constant *εreff*is expressed as,

$$\varepsilon_{reff} = \frac{\varepsilon_r+1}{2} + \frac{\varepsilon_r-1}{2}\left(\frac{1}{\sqrt{1+\frac{12}{W}}}\right) \quad (3.2)$$

where h is the substrate height, the effective length Leff is obtained as,

$$L_{eff} = \frac{c}{2fr\sqrt{\varepsilon_{reff}}} \quad (3.3)$$

Patch's actual length is estimated using the equation 4

$$L = L_{eff} - 2\Delta L \quad (3.4)$$

where ΔL is extension length of the patch and is given by,

$$\Delta L = 0.412h\frac{(\varepsilon_{reff}+0.3)\left(\frac{W}{h}+0.264\right)}{(\varepsilon_{reff}-0.258)\left(\frac{W}{h}+0.8\right)} \quad (3.5)$$

There are number of feeding techniques present in operating an antenna such as aperture-coupled coaxial feed, proximity-coupled feed, inset feed, microstrip feed, and coplanar waveguide feed. Any of these techniques can be used ensuring the efficient power transfer between the

The proposed dual-band antenna system integrates a sub-6 GHz elliptical patch resonator with a millimeter-wave cylindrical dielectric resonator to achieve simultaneous operation across microwave and mm-wave bands. The elliptical patch, designed for the lower band, incorporates a circular hollow at its center to accommodate the CDRA without significantly altering its resonant frequency. To restore the patch resonance, the dimensions are optimized, and a rectangular slot is added to enhance radiation. The mm-wave CDRA, made of commercially available dielectric material, is designed for high-gain operation and initially analyzed as a standalone element. The two resonators are combined to form a compact, integrated structure, enabling dual-band operation. To suppress unwanted harmonics of the lower band and improve isolation between bands, a low-pass filter is incorporated with the sub-6 GHz patch, ensuring efficient and interference-free performance across both frequency ranges.

International Journal of Engineering & Extended Technologies Research (IJEETR)

|ISSN: 2322-0163| www.ijeetr.com | A Bimonthly, Peer Reviewed, Scholarly Indexed Journal |

| Volume 8, Issue 2, March - April 2026 |

DOI:10.15662/IJEETR.2026.0802126

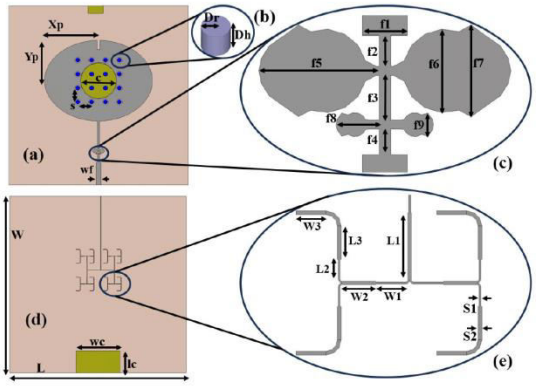

Fig:1 Structural configuration of the proposed antenna (a) front view, (b) DRA, (c) LPF, (d) back view, (e) feeding network.

W = 100, L = 100, wc= 30, lc = 15, Xp= 36, Yp= 27, c = 24, s = 9, wf= 3.1, Dr = 1.5, Dh = 2.2, L1 = 4.45, L2 = 1.3, L3 = 2.2, W1 = 2.0, W2 = 2.2, W3 = 2.0, S1 = 0.13, S2 = 0.25, f1 = 1.5, f2 = 1.0, f3 = 1.5, f4 = 0.85, f5 = 3.8, f6 = 2.65, f7 = 2.9, f8 = 1.36, f9 = 0.75.(all dimensions in millimetre).

IV. ANTENNA CONFIGURATION AND PROPOSED SYSTEM

The proposed dual-band high-gain hybrid antenna consists of two main resonators placed on a two-layer Rogers RO3003 substrate of dimensions 100 × 100 mm² and relative permittivity $\varepsilon_r = 3$. The antenna is designed to simultaneously support microwave (sub-6 GHz) and millimeter-wave (mm-wave) communication. The design process is divided into four main modules for clarity:

A. Elliptical Patch Resonator for Sub-6 GHz Band

The first module is the elliptical patch resonator, designed to operate in the sub-6 GHz band. The resonator is excited in the TM $_{11}$ mode, providing the fundamental resonance. The effective semi-major axis of the elliptical patch is calculated using:

$$\left(x_p = x_p \left[1 + \frac{2h}{\pi \varepsilon_r x_p} \left\{ \left| \ln\left(\frac{x_p}{2h}\right) + (1.77 + 1.41\varepsilon_r) \frac{x_p}{h(1.65 + 0.268\varepsilon_r)} \right\} \right] \right)^{1/2}$$

where:

- x_p– Semi-major axis of the patch
- h– Thickness of the substrate
- ε_r– Dielectric constant of the substrate

The resonant frequency of the elliptical patch is given by:

$$f_{e,o}^{11} = \frac{15}{\pi \varepsilon_r x_p} \sqrt{q_{e,o}^{11}}$$

where $q_e^{11}$and $q_o^{11}$are the approximate Mathieu functions for the TM $_{11}$ mode:

$$q_e^{11} = 0.005e + 3.789e^2 - 0.729e^3 + 2.31e^4$$

$$q_o^{11} = 0.00631e + 3.832e^2 - 1.135e^3 + 5.223e^4$$

Here, $e$represents the eccentricity of the ellipse.

The elliptical patch is modified to include a circular hollow at its center to accommodate the mm-wave CDRA. This introduces a shift in the resonant frequency, which is compensated by slightly adjusting the patch dimensions. Additionally, a rectangular slot is etched on the patch to enhance the radiating area and restore resonance while maintaining bandwidth.

|ISSN: 2322-0163| www.ijeetr.com | A Bimonthly, Peer Reviewed, Scholarly Indexed Journal |

| Volume 8, Issue 2, March - April 2026 |

DOI:10.15662/IJEETR.2026.0802126

B. Cylindrical Dielectric Resonator Antenna (CDRA) for mm-Wave Band

The second module is the Cylindrical Dielectric Resonator Antenna (CDRA), designed for mm-wave operation. The CDRA is placed in the hollow of the patch and made of Hik500 material with $\varepsilon_r = 10$and low loss tangent, chosen for cost-effectiveness and commercial availability.

The resonator dimensions—height $D_h$and radius D_r—are estimated using:

$$f = \frac{30k_0D_r}{2h\left(\frac{D_r}{D_h}\right)}$$

where:

- k_0– Free-space wavenumber
- D_r/D_h– Aspect ratio of the cylindrical resonator

For the fundamental TE $_{011}$ mode, $k_0D_r$is calculated as:

$$k_0D_r = \frac{1}{\sqrt{\varepsilon_r + 1}}\left(1 - 0.00271\left(\frac{D_r}{D_h}\right)^2 + 0.701\frac{D_r}{D_h}\right)$$

These equations provide initial estimates for the CDRA dimensions. However, they do not account for the excitation network effects and the finite ground plane, which are considered during full-wave simulation to fine-tune the resonance and bandwidth.

C. Dual-Band Integration

Once the individual modules are designed, they are integrated into a hybrid patch-CDRA structure. The elliptical patch forms the lower band radiator, while the CDRA is inserted into the patch's hollow to form the mm-wave radiating element.

Key design considerations include:

1. Resonance alignment: The hollow shifts the patch resonance, which is compensated by resizing the patch and adding a slot.
2. Isolation: Careful placement ensures minimal coupling between sub-6 GHz and mm-wave elements.
3. Radiation efficiency: Both elements are optimized for maximal realized gain and wide bandwidth in their respective bands.

The combined structure is simulated using full-wave solvers, and the S-parameters for each band are verified separately before full integration.

D. Low-Pass Filter (LPF) for Harmonic Suppression

To suppress unwanted harmonics generated by the patch resonator and improve isolation between the sub-6 GHz and mm-wave bands, a low-pass filter is incorporated with the patch antenna. The LPF can be modeled using a π-section LC network, where the cutoff frequency $f_c$is designed below the mm-wave band:

$$f_c = \frac{1}{2\pi\sqrt{LC}}$$

where:

- L– Series inductance
- C– Shunt capacitance

This ensures that higher-order harmonics of the patch are suppressed, while the fundamental resonance of the sub-6 GHz band remains unaffected. The LPF improves dual-band isolation and overall antenna performance.

V. SIMULATION RESULTS

International Journal of Engineering & Extended Technologies Research (IJEETR)

|ISSN: 2322-0163| www.ijeetr.com | A Bimonthly, Peer Reviewed, Scholarly Indexed Journal |

| Volume 8, Issue 2, March - April 2026 |

DOI:10.15662/IJEETR.2026.0802126

The simulation settings within HFSS are carefully configured to replicate real-world conditions, ensuring the accuracy and reliability of the results. Parameters such as frequency range, mesh size, and boundary conditions are adjusted to achieve desired simulation outcomes. Additionally, the simulation environment is configured to mimic the antenna's surroundings, such as an open-air or enclosed environment, to evaluate its performance in different scenarios.

After setting up the simulation environment, the proposed patch antenna model is analyzed for various performance metrics, including gain, Voltage Standing Wave Ratio (VSWR), and Return Loss (RL). These metrics provide valuable insights into the antenna's efficiency, bandwidth, and impedance matching capabilities. Through rigorous analysis and optimization, the antenna design is refined to meet specified performance criteria and application requirements.

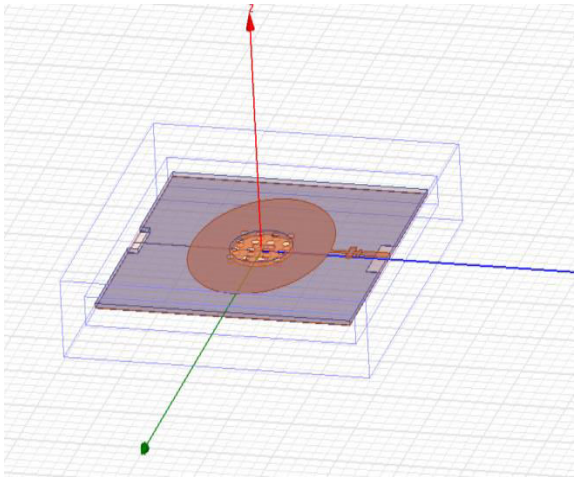

Fig 5.1 Proposed structure

The above figure shows the radiating element design of proposed antenna. In radiator , the cuts are created to tuned for the required frequency . The radiator is formed on substrate.

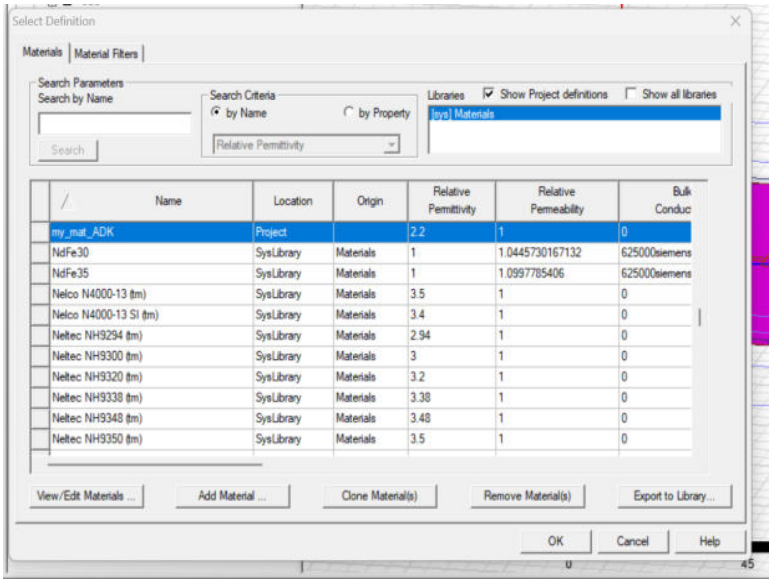

Fig.5.2 Material design

The above figure shows rogers substrate design for proposed antenna design. By using film technology the proposed antenna mounted on rogers substrate .

International Journal of Engineering & Extended Technologies Research (IJEETR)

|ISSN: 2322-0163| www.ijeetr.com | A Bimonthly, Peer Reviewed, Scholarly Indexed Journal |

| Volume 8, Issue 2, March - April 2026 |

DOI:10.15662/IJEETR.2026.0802126

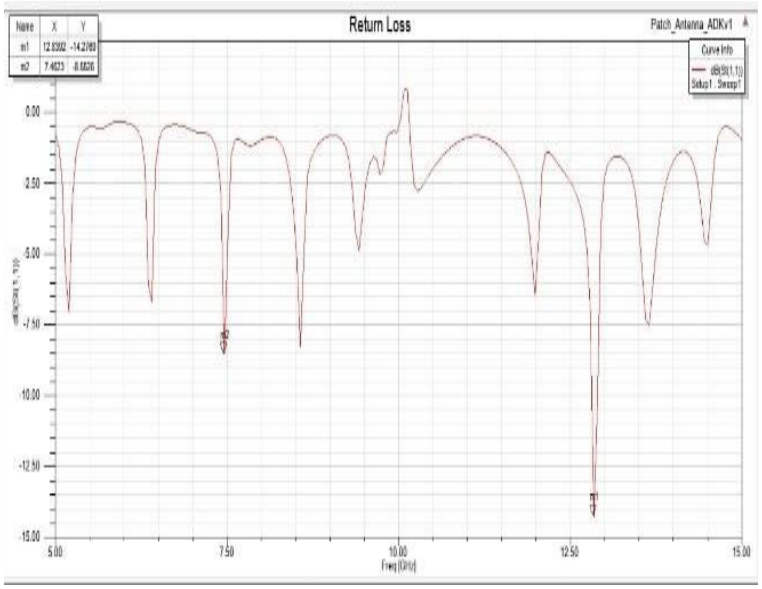

Fig 5.3 Return loss

The above figure shows the return loss analysis of proposed antenna. The proposed antenna achieved a RL of 12.83dB with the tuned frequency .The effect of creating various slots analyzed for different cuts in a radiating elements.

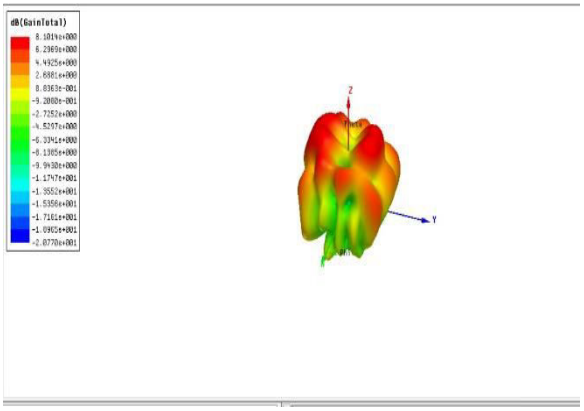

Fig 5.4 3D Gain

Figure shows the gain analysis of proposed antenna. The proposed model achieved a gain value of 8dBfor the tuned frequency. The average values of gain achieved about 8dB in the rogers substrate.

International Journal of Engineering & Extended Technologies Research (IJEETR)

|ISSN: 2322-0163| www.ijeetr.com | A Bimonthly, Peer Reviewed, Scholarly Indexed Journal |

| Volume 8, Issue 2, March - April 2026 |

DOI:10.15662/IJEETR.2026.0802126

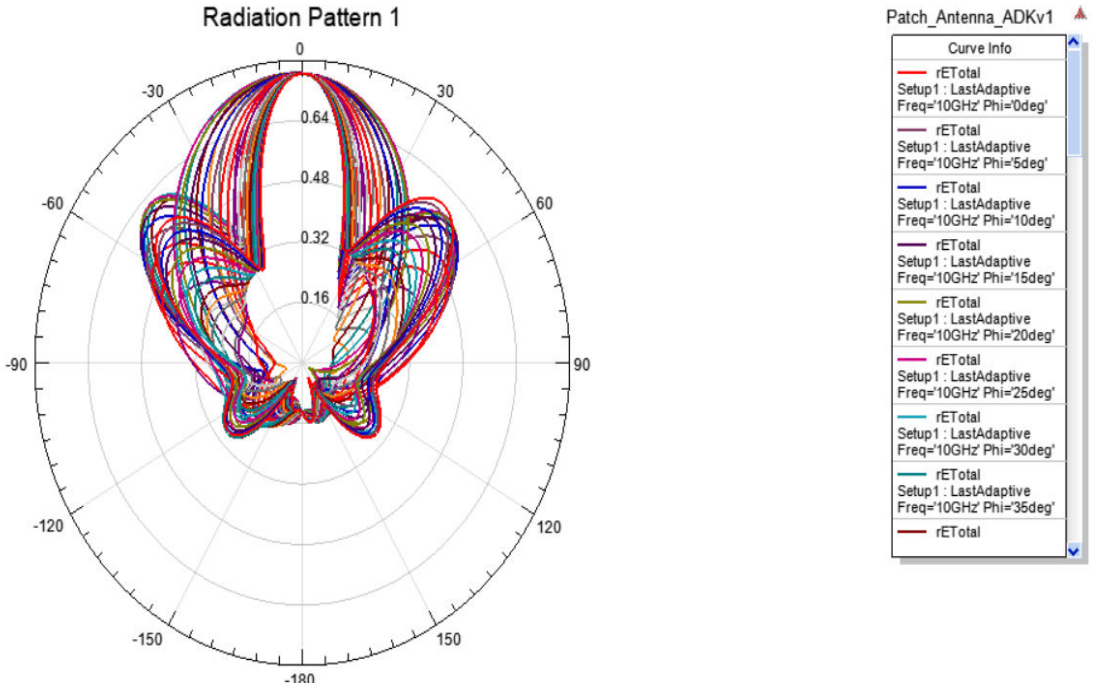

Figure: 5.5 Radiation pattern of proposed antenna

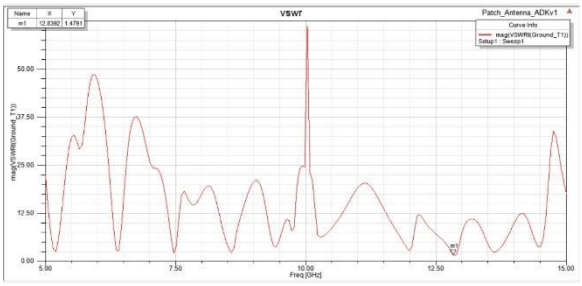

Figure: 5.6 VSWR measurement

Table 1: Performance analysis

Parameter	Existing	Proposed
Return Loss	11.88dB	12.83dB
Gain	6dB	8dB

|ISSN: 2322-0163| www.ijeetr.com | A Bimonthly, Peer Reviewed, Scholarly Indexed Journal |

| Volume 8, Issue 2, March - April 2026 |

DOI:10.15662/IJEETR.2026.0802126

The Reflection Coefficient (RL) is a critical parameter used to evaluate the impedance matching of an antenna. In the simulation results, a RL of 12.83 dB was observed. This RL value is highly indicative of excellent impedance matching characteristics.

A RL of 12.83 dB represents a very low level of reflection. It means that the antenna design is effectively transferring almost all of the power from the source into radiated signals, with very little being reflected back. This is a remarkable outcome as it signifies that the antenna is well-tuned to the operating frequency, minimizing signal loss due to impedance mismatch.The Gain of the antenna is a key performance metric that quantifies its ability to direct and focus radiation in a specific direction. In this simulation, a Gain of 8 dB was observed.

A Gain of 8 dB is a strong indicator of the antenna's ability to concentrate and direct radiation efficiently. It is a positive value, indicating that the antenna is capable of concentrating radiation energy in a particular direction. This directional gain is highly desirable in applications where signal strength and coverage are essential. In summary, the HFSS simulation results with a RL of 12.83 dB and a Gain of 8dB demonstrate that the designed Antenna is an exceptional performer. The RL value of 12.83 dB suggests outstanding impedance matching, minimizing signal loss and ensuring efficient power transfer. Meanwhile, the Gain of 8 dB highlights the antenna's directional radiation capabilities, making it a promising choice for applications that require high-performance antennas, including modern wireless communication systems and radar technologies.

VI. CONCLUSION

A compact dual-band hybrid antenna system has been proposed, integrating a sub-6 GHz elliptical patch resonator with a millimeter-wave cylindrical dielectric resonator array. The design demonstrates simultaneous operation in both microwave and mm-wave bands while maintaining high realized gain and wide bandwidth. The elliptical patch incorporates a central hollow and a slot to accommodate the CDRA and restore resonance, while a low-pass filter effectively suppresses unwanted harmonics and improves band isolation. The mm-wave CDRA is configured as a multi-element array to achieve high-gain radiation suitable for long-distance communication. The proposed design offers independent control of each frequency band, reduced overall size, and enhanced dual-band performance, making it suitable for next-generation wireless communication systems that require simultaneous sub-6 GHz and mm-wave operation.

REFERENCES

1. Zou, H., Li, Y., Shen, H., Wang, H., & Yang, G. (2017). Design of 6 × 6 dual-band MIMO antenna array for 4.5G/5G smartphone applications. 2017 Sixth Asia-Pacific Conference on Antennas and Propagation (APCAP).
2. He, Y., Lv, S., Zhao, L., Huang, G.-L., Chen, X., & Lin, W. (2021). A Compact Dual-Band and Dual-Polarized Millimeter-Wave Beam Scanning Antenna Array for 5G Mobile Terminals. IEEE Access, 9, 109042–109052.
3. Zhu, L., Hwang, H., Ren, E., & Yang, G. (2017). High performance MIMO antenna for 5G wearable devices. 2017 IEEE International Symposium on Antennas and Propagation & USNC/URSI National Radio Science Meeting
4. Kim, G., & Kim, S. (2021). Design and Analysis of Dual Polarized Broadband Microstrip Patch Antenna for 5G mmWave Antenna Module on FR4 Substrate. IEEE Access, 9, 64306–64316.
5. Valkonen, R., &Doumanis, E. (2019). Analysis and design of mm-wave phased array antennas for 5G access. 2019 IEEE International Symposium on Antennas and Propagation and USNC-URSI Radio Science Meeting.
6. Chattha, H. T. (2019). 4-Port 2-Element MIMO Antenna for 5G Portable Applications. IEEE Access, 1–1.
7. Chen, Y., Wang, M., Yi, Z., Zhang, R., & Yang, G. (2019). A Wide-beamwidth Dual-band L-probe Fed Antenna with Parasitic Posts for 5G Communication. 2019 International Applied Computational Electromagnetics Society Symposium - China (ACES).
8. Alja'afreh, S. S., Altarawneh, B., Alshamaileh, M. H., Almajali, E. R., Hussain, R., Sharawi, M. S., … Xu, Q. (2021). Ten Antenna Array Using a Small Footprint Capacitive-Coupled-Shorted Loop Antenna for 3.5 GHz 5G Smartphone Applications. IEEE Access, 9, 33796–33810.
9. C.Nagarajan and M.Madheswaran - 'Stability Analysis of Series Parallel Resonant Converter with Fuzzy Logic Controller Using State Space Techniques'- Taylor &Francis, Electric Power Components and Systems, Vol.39 (8), pp.780-793, May 2011. DOI: 10.1080/15325008.2010.541746
10. C.Nagarajan and M.Madheswaran - 'Experimental verification and stability state space analysis of CLL-T Series Parallel Resonant Converter' - Journal of Electrical Engineering, Vol.63 (6), pp.365-372, Dec.2012. DOI: 10.2478/v10187-012-0054-2

|ISSN: 2322-0163| www.ijeetr.com | A Bimonthly, Peer Reviewed, Scholarly Indexed Journal |

| Volume 8, Issue 2, March - April 2026 |

DOI:10.15662/IJEETR.2026.0802126

11. C.Nagarajan and M.Madheswaran - 'Performance Analysis of LCL-T Resonant Converter with Fuzzy/PID Using State Space Analysis'- Springer, Electrical Engineering, Vol.93 (3), pp.167-178, September 2011. DOI 10.1007/s00202-011-0203-9
12. S.Tamilselvi, R.Prakash, C.Nagarajan,"Solar System Integrated Smart Grid Utilizing Hybrid Coot-Genetic Algorithm Optimized ANN Controller" Iranian Journal Of Science And Technology-Transactions Of Electrical Engineering, DOI10.1007/s40998-025-00917-z,2025
13. S.Tamilselvi, R.Prakash, C.Nagarajan," Adaptive sliding mode control of multilevel grid-connected inverters using reinforcement learning for enhanced LVRT performance" Electric Power Systems Research 253 (2026) 112428, doi.org/10.1016/j.epsr.2025.112428
14. S.Thirunavukkarasu, C. Nagarajan, 2024, "Performance Investigation on OCF and SCF study in BLDC machine using FTANN Controller," Journal of Electrical Engineering And Technology, Volume 20, pages 2675–2688, (2025), doi.org/10.1007/s42835-024-02126-w
15. C. Nagarajan, M.Madheswaran and D.Ramasubramanian- 'Development of DSP based Robust Control Method for General Resonant Converter Topologies using Transfer Function Model'- *Acta Electrotechnica et Informatica Journal* , Vol.13 (2), pp.18-31,April-June.2013, DOI: 10.2478/aeei-2013-0025.
16. C.Nagarajan and M.Madheswaran - 'DSP Based Fuzzy Controller for Series Parallel Resonant converter'- *Springer, Frontiers of Electrical and Electronic Engineering*, Vol. 7(4), pp. 438-446, Dec.12. DOI 10.1007/s11460-012-0212-0.
17. C.Nagarajan and M.Madheswaran - 'Experimental Study and steady state stability analysis of CLL-T Series Parallel Resonant Converter with Fuzzy controller using State Space Analysis'- *Iranian Journal of Electrical & Electronic Engineering*, Vol.8 (3), pp.259-267, September 2012.
18. C.Nagarajan and M.Madheswaran, "Analysis and Simulation of LCL Series Resonant Full Bridge Converter Using PWM Technique with Load Independent Operation" has been presented in ICTES'08, a IEEE / IET International Conference organized by M.G.R.University, Chennai.Vol.no.1, pp.190-195, Dec.2007
19. Suganthi Mullainathan, Ramesh Natarajan, "An SPSS and CNN modelling based quality assessment using ceramic materials and membrane filtration techniques", Revista Materia (Rio J.) Vol. 30, 2025, DOI: https://doi.org/10.1590/1517-7076-RMAT-2024-0721
20. M Suganthi, N Ramesh, "Treatment of water using natural zeolite as membrane filter", Journal of Environmental Protection and Ecology, Volume 23, Issue 2, pp: 520-530,2022
21. Da Costa, I. F., Cerqueira, S. A., &Spadoti, D. H. (2017). Dual-band antenna array with beam steering for mm-waves 5G networks. 2017 SBMO/IEEE MTT-S International Microwave and Optoelectronics Conference (IMOC).
22. Wang, Y.-Y., Ban, Y.-L., & Liu, Y. (2019). Sub-6GHz 4G/5G Conformal Glasses Antennas. IEEE Access, 7, 182027–182036.
23. Wang, Y., Ying, Z., & Yang, G. (2017). A compact CPW-fed wideband antenna design for 5G/WLAN wireless application. 2017 IEEE International Symposium on Antennas and Propagation & USNC/URSI National Radio Science Meeting.
24. Hussain, N., Jeong, M., Park, J., & Kim, N. (2019). Low-Profile Broadband Circularly Polarized Fabry-Perot Resonant Antenna Using A Single-Layered PRS for 5G MIMO Applications. IEEE Access, 1–1.
25. Haskou, A., Pesin, A., Le Naour, J.-Y., &Louzir, A. (2018). Four-Port, Broadband, Compact Antenna for 5G Indoor Access and Content Distribution over WiFi. 2018 International Conference on High Performance Computing & Simulation (HPCS).
26. Hu, H.-N., Lai, F.-P., & Chen, Y.-S. (2020). Dual-Band Dual-Polarized Scalable Antenna Subarray for Compact Millimeter-Wave 5G Base Stations.
27. Gopinathan, V. R. (2025). AI-Powered Kubernetes Orchestration for Complex Cloud-Native Workloads. *International Journal of Research Publications in Engineering, Technology and Management (IJRPETM), 8(6), 13215-13225.*
28. Mathew, A. (2023). Learning Metaverse Powered by Artificial Intelligence. Recent Progress in Science and Technology Vol. 4, 4, 134-141.
29. Garg, V. K., Soundappan, S. J., & Kaur, E. M. (2020). Enhancement in intrusion detection system for WLAN using genetic algorithms. *South Asian Research Journal of Engineering and Technology, 2(6), 62–64. https://doi.org/10.36346/sarjet.2020.v02i06.003*
30. Sugumar, R. (2025). Secure and Explainable AI Systems in Cloud-Based Applications: Bridging Trust and Performance. *International Journal of Engineering & Extended Technologies Research (IJEETR), 7(4), 10328-10335.*
31. Mathew, A., & Alex, H. (2023). From Code to Cure: The Role of AI in Accelerating Drug Discovery. Advances and Challenges in Science and Technology Vol. 2, 94-102.